



# Exploiting the Amazonian Açaí Palm Leaves Potential as Reinforcement for Cement Composites through Alkali and Bleaching Treatments

Carlos Eduardo Gouveia Guedes, Dhimitrius Neves Paraguassú Smith de Oliveira, Jefferson Bezerra Bezerra, Ciro Augusto Fernandes de Oliveira Penido, Nilson Santos Ferreira, Wardsson Lustrino Borges, Lina Bufalino & Tiago Marcolino Souza

To cite this article: Carlos Eduardo Gouveia Guedes, Dhimitrius Neves Paraguassú Smith de Oliveira, Jefferson Bezerra Bezerra, Ciro Augusto Fernandes de Oliveira Penido, Nilson Santos Ferreira, Wardsson Lustrino Borges, Lina Bufalino & Tiago Marcolino Souza (2021): Exploiting the Amazonian Açaí Palm Leaves Potential as Reinforcement for Cement Composites through Alkali and Bleaching Treatments, Journal of Natural Fibers, DOI: [10.1080/15440478.2021.1941483](https://doi.org/10.1080/15440478.2021.1941483)

To link to this article: <https://doi.org/10.1080/15440478.2021.1941483>



Published online: 28 Jun 2021.



Submit your article to this journal [↗](#)



Article views: 62



View related articles [↗](#)



View Crossmark data [↗](#)



# Exploiting the Amazonian Açai Palm Leaves Potential as Reinforcement for Cement Composites through Alkali and Bleaching Treatments

Carlos Eduardo Gouveia Guedes<sup>a</sup>, Dhimitrius Neves Paraguassú Smith de Oliveira<sup>id</sup><sup>a</sup>, Jefferson Bezerra Bezerra<sup>id</sup><sup>a</sup>, Ciro Augusto Fernandes de Oliveira Penido<sup>b</sup>, Nilson Santos Ferreira<sup>id</sup><sup>c</sup>, Wardsson Lustrino Borges<sup>id</sup><sup>d</sup>, Lina Bufalino<sup>id</sup><sup>e</sup>, and Tiago Marcolino Souza<sup>id</sup><sup>f</sup>

<sup>a</sup>Environment Science Department, Federal University of Amapá, Macapá, Brazil; <sup>b</sup>Polícia Técnico-científica do Estado do Amapá, Macapá, Brazil; <sup>c</sup>Physics Department, Federal University of Sergipe, São Cristóvão, Brazil; <sup>d</sup>Embrapa Amapá E Embrapa Agroindústria Tropical, Macapá, Brazil; <sup>e</sup>Agrarian Science Institute, Rural Federal University of Amazonia, Belém, Brazil; <sup>f</sup>Chemical Engineering Department, State University of Amapá, Macapá, Brazil

## ABSTRACT

Recent investigations proposed alternatives for utilization of Açai (*Euterpe oleracea* Mart.) fruit wastes, seeds, and lignocellulosic fibers. However, Açai leaves may also be obtained without harvesting the palms and could be used in higher value-added products. Alkali reaction (1% and 5% of NaOH), different temperatures (70°C, 80°C, and 100°C), and bleaching were combined to produce fibres from the Açai leaves. Scanning electron microscopy, X-ray diffraction, and thermogravimetry were used to evaluate the effect of treatments on fibers, whereas X-ray diffraction and calorimetry were employed to characterize Portland cement pastes containing fibers. Results indicated that Açai leaves could be transformed into short-length fibers with improved degrading temperature. Alkali treatment at 5% sodium hydroxide (90°C) and bleaching increased fibers' crystallinity and showed efficiency in removing non-cellulosic components. Cement paste evaluation also indicated that fibers treated at 5% NaOH solution caused fewer changes in calorimetric profile and therefore present a greater potential for cement-based composites.

## 摘要

最近的调查提出了一种新的能源利用方法 Açai (果实废料、种子和木质纤维)。然而,也可以不收割棕榈而获得 Açai 叶,并且可以用于高附加值产品。碱反应(1%和5%氢氧化钠),不同温度(70°C、80°C、和100°C),和漂白相结合,从 Açai 树叶。扫描电子显微镜、X射线衍射和热重分析用于评估处理对纤维的影响,而X射线衍射和量热分析用于表征含有纤维的硅酸盐水泥浆体。结果表明, Açai 随着降解温度的提高,叶片可以转化为短纤维。5%氢氧化钠(90°C)碱处理提高了纤维的结晶度,对非纤维素组分有较好的去除效果。水泥浆体评价还表明,在5%NaOH溶液中处理的纤维对量热曲线的影响较小,因此对水泥基复合材料具有更大的潜力。

## KEYWORDS

Biomass; fiber morphology; thermal stability; biocomposite; ceramic-matrix; Portland cement

## 关键词

生物量; 纤维形态; 热稳定性; 生物复合材料; 陶瓷基体; 硅酸盐水泥

## Introduction

The growing demand for green and environmentally sustainable materials and processes has stimulated research in different engineering areas. Such worry and current environmental control legislation have also driven the primary sector to replace polluting materials and nonrenewable sources (Leão et al. 2007).

**CONTACT** Tiago Marcolino Souza ✉ [uaitiago@gmail.com](mailto:uaitiago@gmail.com) 📧 Chemical Engineering Department, State University of Amapá, 650 Presidente Vargas Av. 68, Macapá, 900-070, Brazil

© 2021 Taylor & Francis

Due to their cost-effective benefits compared to synthetic fibers, there is considerable interest in using natural fibers to substitute reinforcements like asbestos, fiberglass, and steel (Yan, Kasal, and Huang 2016). In the case of cement-based materials, for example, several advantages are reported for the use of natural fibers, as better mechanical performance, flexural strength, toughness, and impact resistance (Bilba and Arsene 2008; Pacheco-Torgal and Jalali 2011). Besides, they are degradable and eco-friendly and can be easily disposed of at the end of their life cycle (Faruk et al. 2014; Indran and Raj 2015).

Lignocellulosic fibers consist of structural (cellulose, hemicelluloses, and lignin) and non-structural (waxes, fatty acids, fats, pectins, minerals, among others) components (Martins, Kiyohara, and Joékes 2004; Rowell, Han, and Rowell 2000). The structural elements compose cell wall structure, whereas non-structural ones are impregnated on the surfaces. Cellulose is a polysaccharide present in greater quantity in the plant cell walls. It is a linear chain biopolymer comprised of glucose monomers linked via  $\beta$ -(1-4) glycosidic bonds. The cellulose molecules are organized side-by-side, forming semicrystalline microfibrils, constituted of major crystalline regions linked by amorphous ones (Ioelovich 2008; Morán et al. 2008; Oksman et al. 2006). Fibers with greater cellulose amount and crystallinity usually present higher stiffness (Cai et al. 2016; Chen et al. 2011). Thus, lignocellulosic fibers' efficiency as reinforcing materials depends mainly on the cellulose structure (Khan and Khan 2015).

Different sorts of lignocellulosic fibers have been investigated as reinforcement components for composites, such as sugarcane bagasse (Hajiha and Sain 2015), sisal, coir, date palm and hemp (Al-Oqla and Sapuan 2014), bamboo (Abdul Khalil et al. 2015), palm leaf (Kocak and Mistik 2015), biomass rejects (César et al. 2019), and others. In general, it is important to investigate the potential of different fibers regarding their physical, chemical, and morphological properties, especially those from renewable sources, and available in large quantities.

A limiting factor to apply plant fibers as reinforcement is their compatibility with the composites' matrix. In the case of cement-bonded materials, incompatibility between lignocellulosic fibers and matrix can generate drawbacks, for example, delay in the cement setting (Macêdo, Souza, and Neto 2012). According to Ferraz et al. (2012), the plant fibers' chemical components as sugars, extractives, hemicelluloses, and lignin are the main ones responsible for such compatibility problems. Some of these components are unstable in the cement hydrating medium, releasing sugars or acid compounds, reducing hydration, setting, and matrix hardening. Consequently, their partial or total elimination from biomass might lead to substantial improvements in cement composite properties (Vo and Navard 2016). The hydroxyl groups available on the surface of remaining cellulose fractions are responsible for fillers and cement bonds (Vo and Navard 2016). Chemical and physical pretreatments of lignocellulosic fibers may reduce incompatibility between the reinforcement and cement matrix. Fiber modification with alkali solution and bleaching is commonly described as efficient methods to improve the lignocellulosic fibers' compatibility (Mohanty, Misra, and Drzal 2005). Variations in NaOH solution concentration and temperature of reaction are usually combined to remove non-cellulosic components from fibers. Besides raising cellulose proportion, alkali and bleaching treatments cause fiber morphological changes, like diameter decrease, individualization from bundles, and individual integrity maintenance (Pedrazzi et al. 2013). However, the gain or improvement in fiber properties may be accompanied by loss of other critical properties, such as crystallinity and degree of polymerization, which must be monitored (Berto and Arantes 2019).

This study aimed to evaluate Açai palm leaves potential as a reinforcement for cement composites using alkali and bleaching pretreatments. Variations in NaOH concentration and temperature were analyzed, aiming to determine suitable conditions to generate fibers with enhanced properties. Additionally, Portland cement pastes containing treated fibers were also assessed by X-ray diffraction and calorimetry.

## Material and methods

### Materials

The leaves of *Euterpe oleracea* Mart. were collected from palm trees of approximately 3-year old in a private area of Macapá, Amapá, Brazil. The leaflets were separated from the leaves and continuously

washed at room temperature to remove adhered materials. Leaflets' central vein was removed using a stilet, and the remaining parts were cut into pieces of  $1.5 \pm 0.3$  cm in length.

Cement pastes containing fibers were prepared using a high initial strength Portland cement (CP V ARI Campeão®, CRH Sudeste Indústria de Cimentos S. A. – Brazil), according to NBR 5733 classification (Associação Brasileira de Normas Técnicas (ABNT) 1991).

### **Treatments of the Açai leaves**

The Açai leaves were pretreated in alkali solutions under mechanical stirring (700 rpm) during 1 h of reaction. Tested conditions combined two NaOH (Sodium Hydroxide P.A. 98%, Dinâmica, Dinâmica Química Contemporânea Ltda) solution concentrations (1% and 5%), three reaction temperatures (70°C, 80°C, and 100°C), and a fiber/solution proportion of 20:1 (g/L). After treatments, solutions containing fibers were filtered in a sieve, washed in distilled water, defibrillated for 1 min in a blender (3500 rpm), and washed again until the distilled water become colorless and reach pH 7.0. Then, the fiber mass was dried at 50°C for 48 h and disaggregated in a blender for 1 min (1200 rpm).

Part of the fibers pretreated in a 5% NaOH solution at 90°C was bleached through immersion in a solution 1:1 (v/v) of H<sub>2</sub>O<sub>2</sub> at 25% (Hydrogen Peroxide 35% v/v P.A., Dinâmica, Dinâmica Química Contemporânea Ltda) and NaOH at 4%. The bleaching was carried out using a fiber/solution proportion of 10:1 (g/L), for 2 h, at 60°C, and under mechanical stirring (800 rpm). After the treatment, fibers were continuously washed in distilled water (until it reaches pH 7.0) and dried at 50°C for 48 h.

### **Cement and cement/fiber paste preparation**

Pastes with a water/cement ratio of 1:3 (w/w) and fiber/cement ratio of 1:20 (w/w) were prepared for X-ray diffraction and semi-adiabatic calorimetry tests. The fiber cement proportion was selected considering fiber density and low-density cement-bonded fiberboards. Aiming to highlight the effect of fiber content, pastes with a water/cement ratio of 1:2.5 (w/w) and fiber/cement ratio of 1:100 (w/w) were also evaluated by calorimetry.

### **Testing procedures**

Fibers' micrographs were obtained in a HITACHI® scanning electron microscope (SEM), TM3030PLUS model, with a voltage of 15 kV. Obtained fibers were evaluated by infrared spectrometry using the attenuated total reflectance (ATR) technique in Spectrum Two™ equipment, Perkin Elmer Instruments®. Thermogravimetric analysis was carried out in an STA 449 F5 Jupiter equipment (Netzsch®), under N<sub>2</sub> atmosphere, from room temperature to 1000°C, using a 10°C/min heating rate. The initial temperature of degradation was considered as the point of intersection between the prolongation of the TG curve (at the constant mass region) and the tangent at the first thermal degradation stage.

The fibers' apparent density was determined adapting NBR 11941 (Associação Brasileira de Normas Técnicas (ABNT) 2003). Tests were conducted using a 10 mL graduated beaker, 6 mL of ethyl alcohol, and 0.1 g of fibers. The diameters of fibers obtained from each treatment were measured using SEM micrographs and the Image J Software. Fibers' density and diameters obtained from the different treatments were evaluated using one-way analysis of variance (ANOVA) and the means compared by the Tukey test, at 5% of significance. Statistical analyses were performed using the OriginPro (Trial License).

The X-ray diffraction patterns were obtained using a Bruker® diffractometer (model D2 Phaser), with Cu K $\alpha$  radiation ( $\lambda = 1.5418$  Å) and nickel filter, a voltage of 30 kV, and 10 mA. Samples were placed on a polymethyl methacrylate holder and analyzed in the  $2\theta$  range varying from 5° to 90°. Phase identification was carried out using a free database. The crystalline fraction of fibers (CF) was

calculated using DIFFRACT.EVA software (Bruker), using the total area below diffractograms between 5° and 45°, after background removal and curve smoothing.

The first XRD analysis of each paste was carried out right after 10 min of the beginning of mixing (considered as the 0 h), aiming to guarantee enough time for sample preparation. Afterward, the paste was removed from the holder and kept inside a zip-locked plastic bag at room temperature. For the analysis after 24 h, it was necessary to crush the samples using a mortar and a pestle.

A semi-adiabatic calorimeter was used to monitor temperature during cement paste hydration. The semi-adiabatic calorimeter was comprised of a plastic thermal box of 26 L, four thermal bottles with an inner glass flask of 250 mL, and four waterproof temperature sensors (DS18B20; 0.5°C of precision between -10 and 85°C) connected to an Arduino micro-controller (Mega 2560 R3) hardware. The samples' components (fiber/cement/water) were mixed and homogenized inside recyclables plastic bags (8 x 5 cm) to produce the pastes. The temperature sensors were introduced into each plastic bag containing the paste. Plastic bags were hermetically sealed, placed into the thermal bottles, stored inside the thermal box, and enveloped with styrofoam. The preparation procedure did not exceed 5 min, and the tests were carried out for 24 h. The average curve of temperature variation as a function of time was determined using four replicates of each cement paste.

## Results and discussion

### *Characterization of the Açai palm leaves and the produced fibers*

Palm leaf visual appearance changes significantly as a consequence of the alkali treatments (Figure 1). The green leaves resulted in fibers of brown and beige coloring with different shades. Fibers produced using the alkali solution at 1%, and lower temperatures were more dispersed and coarser. The treatment at 5% NaOH solution and the temperature increase favors the formation of finer fibers but with more significant aggregation. After bleaching, the fibers' bundles seemed to present lower diameters, lighter coloring, and higher aggregation.

ANOVA results showed significant differences among fibers' diameters for the seven tested conditions (Table 1). The treatments at 5% of NaOH resulted in fibers with lower diameters than

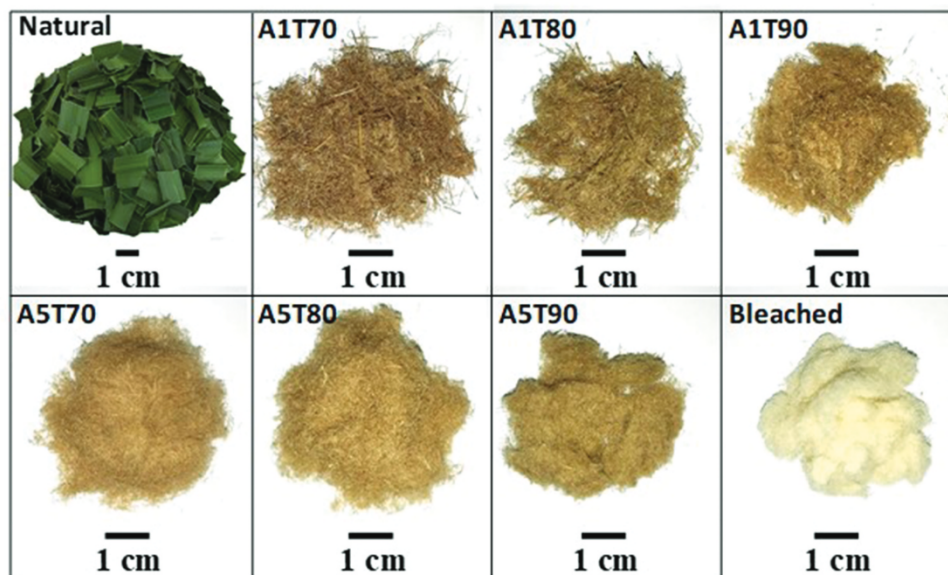


Figure 1. The visual aspect of the natural Açai palm leaves treated with NaOH solution at 1% (A1T70, A1T80, A1T90) and 5% (A5T70, A5T80, A5T90) at 70°C, 80°C and 90°C, and bleached.

the one at 1% (Table 2). According to the Tukey test, the mean diameters formed distinct groups, confirming that temperature and alkali concentration affected fibers' properties. The lowest mean diameter was found for bleached fibers, which did not differ significantly from the ones treated at 5% of NaOH and 90°C. The fibers' density for all treatments was statistically equivalent, approximately  $1.0 \text{ g}\cdot\text{cm}^{-3}$  (Table 2).

Figure 2(a,b) shows the SEM micrographs of the adaxial (superior) and abaxial (inferior) surfaces of natural palm leaves. Açai palm leaves (*Euterpe oleracea* Mart.) epiderm, adaxial, and abaxial surfaces, are generally glabrous and uniseriate (Paula 1975). The epidermal cells have markedly sinuous walls. The adaxial epidermis' cells are broad and moderately elongated, whereas the abaxial epidermis' ones are moderately narrow. Cells of both surfaces are small, with fine pectocellulosic walls, and frequently containing siliceous bodies. As observed by Paula (1975), stomata occur only in the abaxial epidermis, with an irregular distribution (Figure 2(b)).

Natural fibers are oriented and present surfaces covered by a non-uniform layer of amorphous non-cellulosic compounds (like waxes, oil, residual lignin, and impurities) that have a protective function (Rokbi et al. 2011). During the sodium hydroxide solution treatments, hemicelluloses are hydrolyzed and removed, and lignin can be partially degraded (Bufalino et al. 2015). The fibers' surfaces become rougher when these components are removed (Li, Tabil, and Panigrahi 2007). This rougher surface can favor bonding due to hydroxyl groups' exposure to cement matrix, increasing adhesion between cement and fiber (Chikouche et al. 2015; Yan, Chouw, and Yuan 2012). The fibers produced after alkali treatments were heterogeneous, with irregular shape and non-smooth surfaces (Figure 2(c-h)). The increase of NaOH solution concentration (1%, 5%) and temperature (70, 80, 90°C) resulted in finer bundles of fibers and greater individualization.

SEM micrographs of sample A1T80 revealed the presence of small globular particles embedded in pits on surface walls, indicating the presence of siliceous bodies (Figure 3). Globular siliceous-rich compounds were also found recently on the Açai mesocarp fibers (Oliveira et al. 2019). The silica bodies located in stigmata cells are usually associated with poor adhesion when manufacturing composite materials (Luo et al. 2018). The treatment at 5% of NaOH removed some of these siliceous particles and revealed cell structure (A5T80). When compared with fibers treated with 5% of NaOH at 90°C (A5T90), the bleached ones (A5T90B) seem to present cleaner surfaces, poor in non-cellulosic amorphous compounds which typically cover natural leaves (Figure 3).

FT-IR spectra of the Açai palm leaves treated at 1% or 5% NaOH solution and different temperatures are shown in Figure 4. Cellulose's hydroxyl groups (OH) were observed in the spectrum region of  $3200\text{--}3700 \text{ cm}^{-1}$ , whereas the bands associated with methyl's (CH) and methylene's ( $\text{CH}_2$ ) asymmetric

**Table 1.** ANOVA of the fibers' diameters treated at different conditions.

Source	DF	Sum of Squares	Mean Square	F	Data Mean	R-square	CV (%)
Model	6	$2.4864 \times 10^{-8}$	$4.144 \times 10^{-9}$	223.73469	$8.68493 \times 10^{-5}$	0.95517	0.04955
Error	63	$1.16688 \times 10^{-9}$	$1.8522 \times 10^{-11}$	-	-	-	-
Total	69	$2.60309 \times 10^{-8}$	-	-	-	-	-

DF: degree of freedom; CV: coefficient of variation.

**Table 2.** Mean density and diameter of fibers produced at different conditions.

Treatment	Mean density ( $\text{g}/\text{cm}^3$ )	Mean diameter ( $\mu\text{m}$ )
A1T70	$1.01 \pm 0.05$	$105.57 \pm 6.36^a$
A1T80	$1.00 \pm 0.05$	$96.66 \pm 5.80^b$
A1T90	$1.00 \pm 0.05$	$119.47 \pm 4.73^c$
A5T70	$1.01 \pm 0.05$	$75.40 \pm 3.24^d$
A5T80	$1.01 \pm 0.05$	$72.67 \pm 3.35^d$
A5T90	$1.01 \pm 0.05$	$71.57 \pm 2.64^{de}$
Bleached	$1.02 \pm 0.05$	$66.61 \pm 2.10^e$

Means followed by the same case letters within the same column do not differ by Tukey test at 5% significance level.

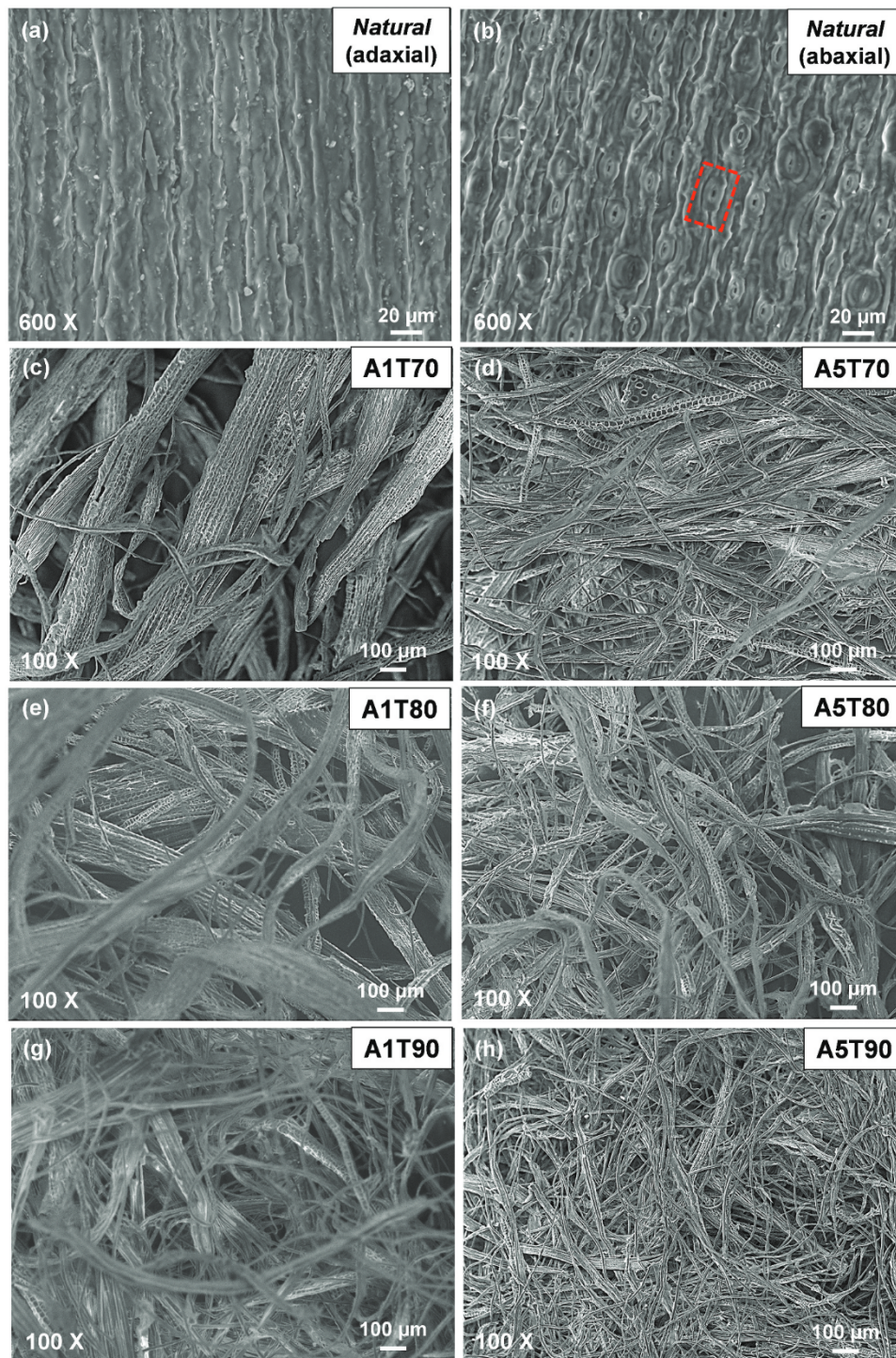


**Figure 2.** Scanning electron micrographs of the natural Açai palm leaves (a-b) and treated (c-h) with NaOH solution at 1% (A1T70, A1T80, A1T90) and 5% (A5T70, A5T80, A5T90) at 70°C, 80°C and 90°C. The selected area in (b) indicates the stomata structure.

stretching were verified around  $2900\text{ cm}^{-1}$  (Gutiérrez et al. 2012; Sgriccia, Hawley, and Misra 2008). The band attributed to the stretching of C-O-C groups (present in hemicelluloses, lignin, and

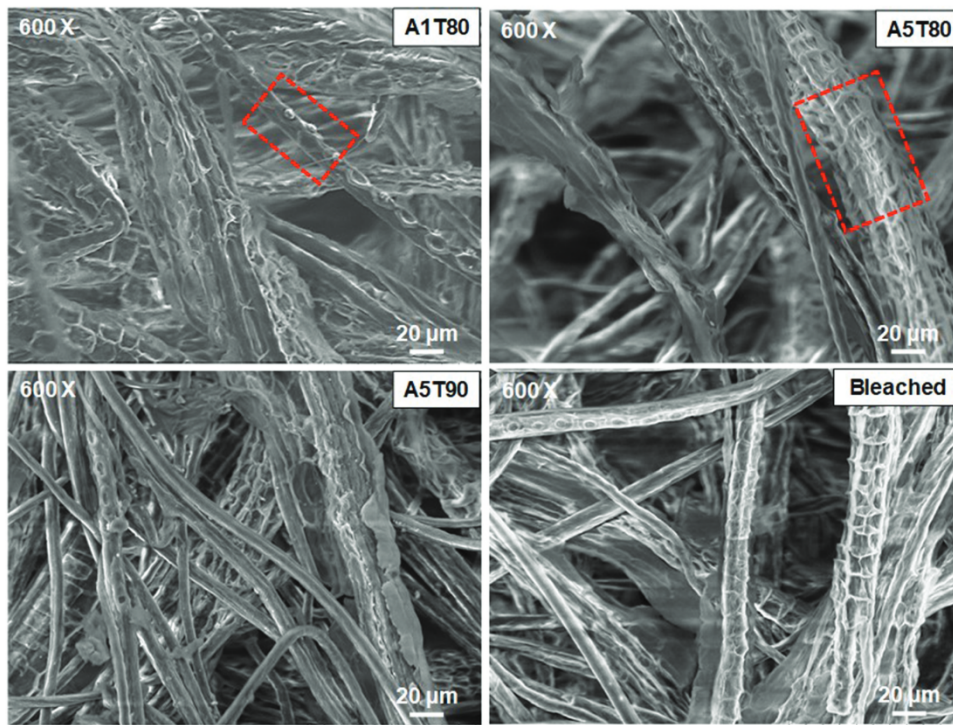


**Figure 3.** Scanning electron micrographs of the Açai palm leaves treated with NaOH solution at 1% and 80°C (A1T80), at 5% and 80°C and 90°C (A5T80, A5T90), and bleached. The selected area in A1T80 indicates the possible siliceous bodies and in A5T80 the cells' cleaner structure, respectively.

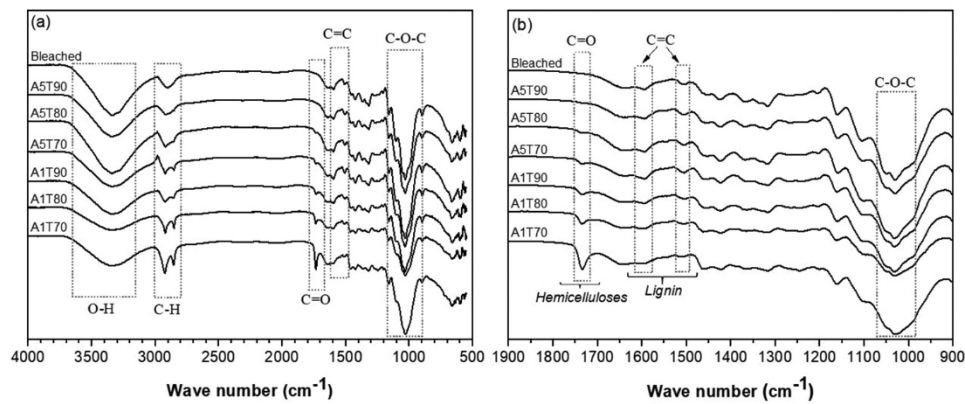


**Figure 4.** FT-IR spectra of (a) the fibers treated with NaOH solution at 1% (A1T70, A1T80, A1T90) and 5% (A5T70, A5T80, A5T90) at 70°C, 80°C and 90°C; and (b) between 1900 and 900  $\text{cm}^{-1}$ .

cellulose) was detected at  $1030 \text{ cm}^{-1}$ , whereas the hemicelluloses' carbonyl ( $\text{C} = \text{O}$ ) one was observed at  $1730 \text{ cm}^{-1}$  (Gutiérrez et al. 2012; Sena Neto et al. 2013). Once this carbonyl band is continuously attenuated for treatments at increasing alkali concentration and temperatures, and it was not detected for bleached fibers, such results indicate that all pretreatments removed hemicelluloses (Figure 4(b)). Vibrations and stretching of  $\text{C} = \text{C}$  groups of the lignin's aromatic ring were verified at  $1590 \text{ cm}^{-1}$  and  $1505 \text{ cm}^{-1}$ , respectively (Bufalino et al. 2015; Sena Neto et al. 2013). Such lignin's bands become slightly intense for fibers treated with higher alkali concentration or bleached, indicating a greater



exposure of the inner lignin (Figure 4(b)). A recent investigation of Açai mesocarp fibers using alkali pretreatments revealed a similar behavior (Oliveira et al. 2019).

XRD diffraction results showed similar patterns for all produced fibers (Figure 5), characteristic of semicrystalline materials. The identified peaks correspond to cellulose I with crystallites preferred orientation along the fiber axis (French 2014). Preferred orientation was confirmed by the absence of peak at  $20.5^\circ$  [(012) and (102) planes] as the smoothed one at  $35.0^\circ$  [(004) plane]. All the treated fibers exhibited a sharp peak at approximately  $22.6^\circ$ , which corresponds to the (200) lattice plane of cellulose I. A band attributed to the overlapping of the celluloses' peaks at  $14.8^\circ$  and  $16.3^\circ$ , assigned to the (1-10) and (110) lattice planes, was also identified (Besbes, Vilar, and Bouf 2011; Klemm et al. 2005).

The XRD results indicated that alkali treatment and bleaching retained the cellulose structure (Figure 5), which is advantageous for fiber application as greater crystallinity is closely related to higher stiffness and better reinforcing efficiency (Chen et al. 2011; Khan and Khan 2015). Treated fibers showed a crystalline fraction (CF) between 30.5% and 40.5% due to the non-cellulosic chemical components' removal, such as extractives, hemicelluloses, and lignin (Corrêa et al. 2010). The alkali reactants reach the cellulose's crystalline surfaces during the treatment, but it seems to penetrate only into disordered regions, whereas the intra-crystalline domains remain unaffected (Ciolacu, Ciolacu, and Popa 2011). Bleaching treatment resulted in a slight decrease in the crystalline fraction compared with A5T90 (Figure 5). Chemical treatments reduce the number of free hydroxyl groups on fibers' surface and, consequently, cellulose molecules' polarity (Kaushik, Kumar, and Kalia 2012). Therefore, the loss of crystallinity may be attributed to the reduction of intra- and intermolecular hydrogen bonds and, consequently, to greater crystalline regions' exposure to degradation (Barneto, Vila, and Ariza 2011; Ciolacu, Ciolacu, and Popa 2011).

Thermal degradation characteristics of the Açai natural leaves and beached fibers are shown in Figure 6. The samples exhibited a decomposition profile characteristic of lignocellulosic materials: moisture loss, hemicellulose decomposition, cellulose decomposition, and a significant temperature range step attributed to lignin (Wilson et al. 2011). DTG curves show an initial peak between 30 and

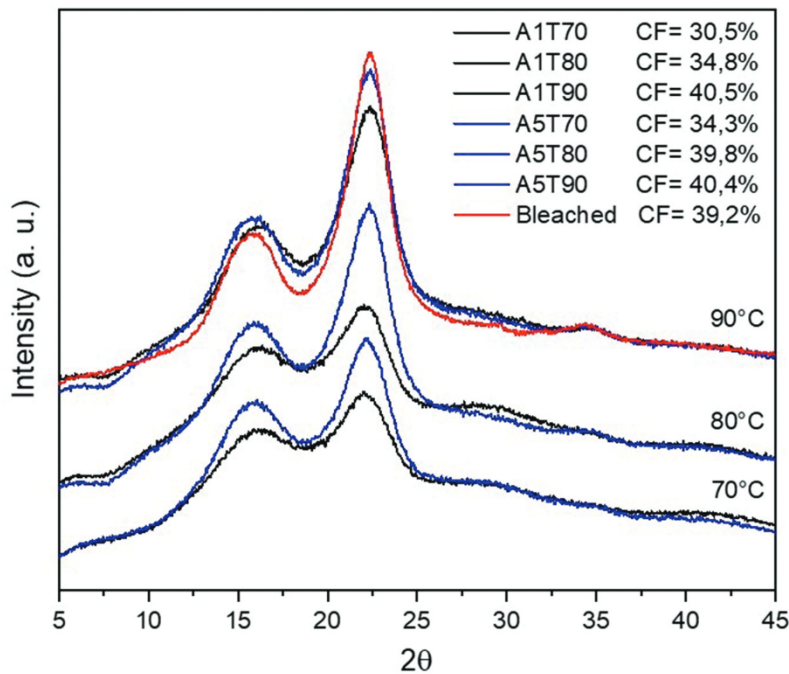
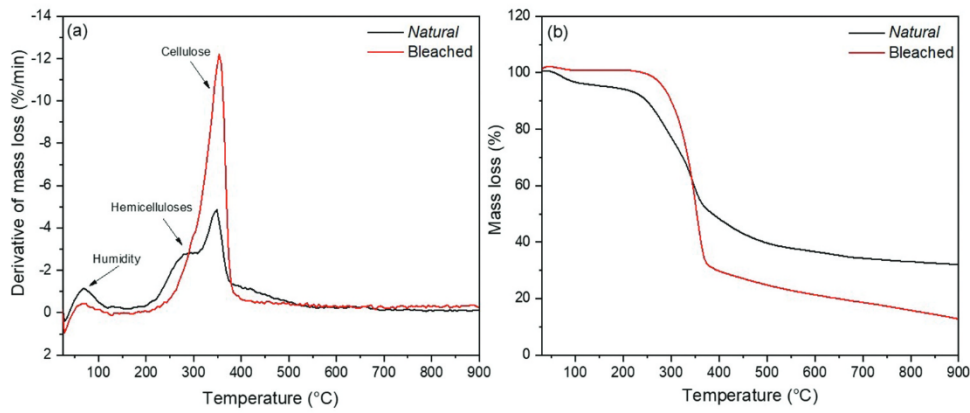


Figure 5. Diffractograms of the fibers treated with NaOH solution at 1% and 5% at  $70^\circ\text{C}$ ,  $80^\circ\text{C}$  and  $90^\circ\text{C}$  (A1T70, A1T80, A1T90, A5T70, A5T80, A5T90) and bleached. CF: Crystalline fraction.



**Figure 6.** Differential thermogravimetric analysis (a) and thermogravimetry (b) under  $N_2$  atmosphere for the natural and bleached fibers.

150°C due to water vapor release and low molecular weight compound decomposition. Mass stabilization occurred earlier for treated fibers, at around 100°C, indicating a lower moisture content (<0.5%) compared to the natural one (~3.22%). Natural and bleached samples start to decompose approximately at 244°C and 378°C, respectively. Since biomass degradation is an irreversible process, this temperature range can be considered as the limit working temperature (Sena Neto et al. 2013). As thermal analyses were conducted under an inert atmosphere, variations in the initial temperature of degradation can be associated with differences in samples' chemical composition (Mansaray and Ghaly 1998). The major mass loss of natural leaves and treated fibers finished at approximately 386°C and 371°C, respectively. During this stage, the degradation of hemicelluloses and cellulose is observed (Figure 6(a)), confirming treatments' effectiveness to remove non-cellulosic components. According to Zhao et al. (2008), treatments with sodium hydroxide solution can slightly remove hemicelluloses, cellulose, and lignin from lignocellulosic materials. The appearance of curve shoulders before and after cellulose degradation peak should correspond to remaining hemicelluloses and lignin, respectively. After the cellulose degradation stage, a continuous mass loss is observed due to the degradation of lignin. At 900°C, the natural fibers still show 32% of residue, whereas the bleached sample presents only 12.5% of the total mass.

### **Cement pastes containing fibers**

According to the literature, one of the main problems affecting the compatibility between Portland cement and lignocellulosic fibers is the content and sort of extractives, especially those with phenolic structures, which usually results in hydration delay and/or inhibition (Na et al. 2014). X-ray diffraction analysis of the cement pastes right after mixing (0 h) and after 24 h was performed to verify fiber addition effects on the formation of hydrated phases (Figure 7).

When compared with the neat cement paste (Figure 7(a)), all fiber-cement ones presented a higher drop of the anhydrous characteristic peaks (like alite and belite) and a relatively higher intense portlandite peak (Figure 7(b,c)). Such behavior is not associated with greater hydration but is a consequence of the difference between the sample's preparation process. Due to faster hardening, the neat cement paste was removed from the sample holder without disintegration. In contrast, the fiber-containing samples disintegrated and required further maceration for the analysis after 24 h. Therefore, the greater intensity of the portlandite peak around 18° may be related to its [001] preferred-orientation axis (Aranda, De la Torre, and León-Reina 2019). Despite that, XRD results allowed a qualitative comparison between cement pastes and

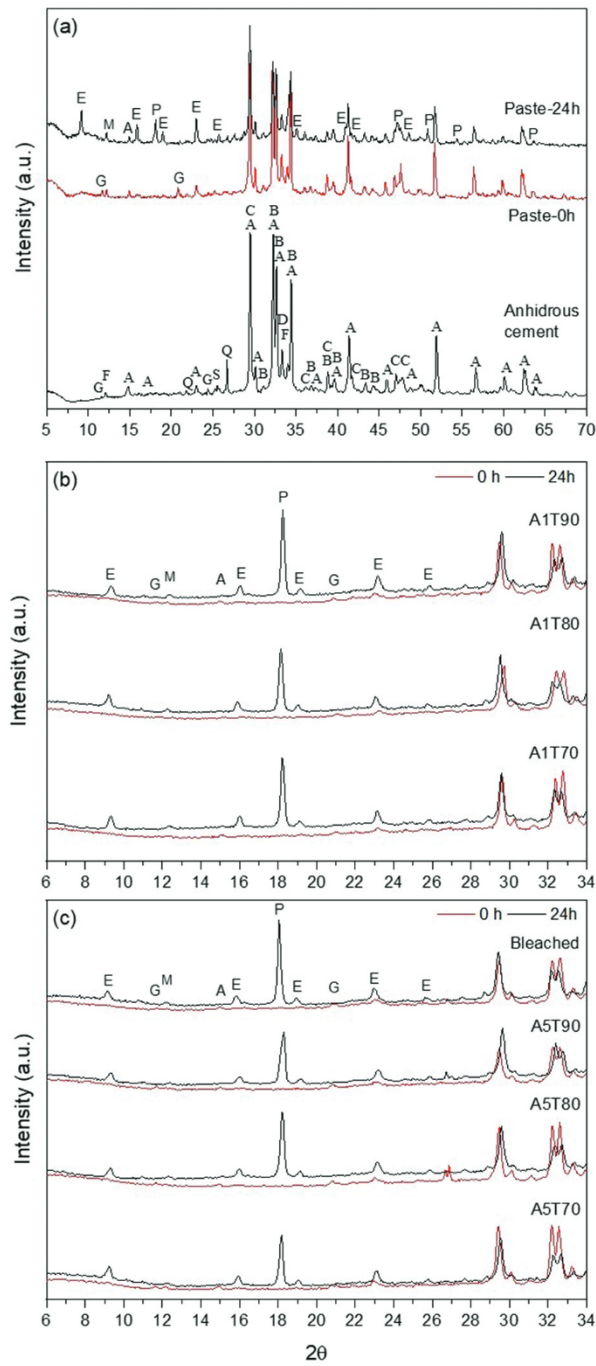


**Figure 7.** XRD results of the anhydrous cement, cement paste right after mixing (0h), and after 24h (a); cement pastes containing fibers treated with NaOH solution at 1% (b) and 5% (c) at different temperatures; and a cement pastes containing bleached fibers. A: alite; B: belite; C: calcite; D: calcium aluminate; E: ettringite; F: brownmillerite; G: gypsum; S: calcium sulfate; Q: quartz; M: calcium monocarboaluminate; P: Portlandite.

confirmation of main hydrated phases (portlandite and ettringite) in the fiber-containing samples (Figure 7(b,c)).

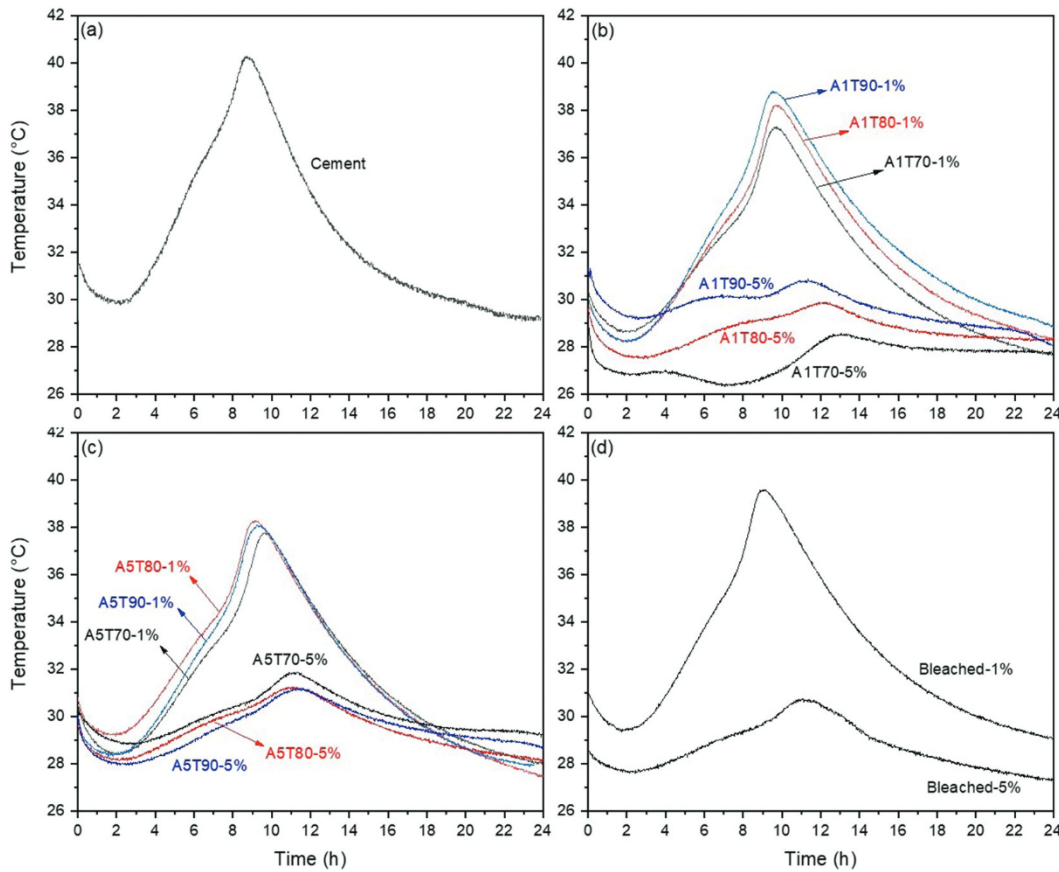


**Figure 8.** Semi-adiabatic calorimetry of the hydrated cement pastes: (a) neat cement; (b) containing 1% and 5% of A1T70, A1T80, or A1T90 fibers; (c) containing 1% and 5% of A5T70, A5T80 or A5T90; and (d) containing bleached fibers.

Semi-adiabatic calorimetry was used to evaluate the hydration kinetics of pastes containing fibers. The inhibition effect usually results in a reduction of maximum hydration temperature and/or a time delay to reach this temperature (Hachmi et al. 2017). When compared to the neat cement (Figure 8 (a)), pastes containing 1% of treated fibers showed very similar curves' profiles with a slight drop and delay in the maximum temperature peak (Figure 8(b-d)). On the other hand, cement pastes containing 5% of fibers indicated a significant drop and delay of the hydration exothermic peak.

For fibers treated at 1% NaOH solution (Figure 8(b)), temperature increase reduces the drop and shifts the maximum temperature peak. At a higher NaOH concentration (5%), the rise in treatment temperature was less significant and resulted in a non-well-defined pattern (Figure 8(c,d)). During cement hydration, the aqueous medium becomes more alkali; consequently, some of the fibers' chemical components can be degraded and released into the medium. The cement hydration rate may be slowed when the positively charged surfaces of the calcium silicate hydrates are disturbed by layers of sugar-acid anions (Garcez et al. 2016; Gartner et al. 2002; Juenger and Jennings 2002). The treatment at 5% NaOH solution removed more extractives and hemicelluloses (Figure 4); consequently, the resultant fibers caused less disruption in cement hydration, as verified in calorimetry tests (Figure 8). Despite the changes in cement hydration profile after fibers' addition, all samples indicated a visible hardening after 24 h of testing, showing that future mechanical investigations could provide helpful information about the feasibility of developing Açai leaf fiber cement-composites.

## Conclusions


Açaí palm leaves were successfully used to produce short-length fibers with reinforcement potential for cement composites. Alkali treatments showed to be efficient in removing the non-cellulosic components and increase fibers' crystallinity. The higher NaOH concentration and temperature favor the formation of finer fibers with apparently rougher and cleaner surfaces. The additional bleaching treatment successfully removed the hemicelluloses and lignin generating fibers with improved degrading temperature.

X-ray diffraction and semi-adiabatic calorimetry results indicated that although cement hydration kinetics was affected by the presence of fibers, the main hydrated phases were detected for all pastes containing Açaí leaf fibers. Fibers treated with NaOH solution at 5% caused fewer changes on pastes' exothermic profile, indicating better perspectives for cement-bonded composites.

## Acknowledgments

The authors are grateful to the Amapá Research Foundation (FAPEAP) for the financial support (First Projects Program – Process Number 250.203.044/2017), to the Coordination for the Improvement of Higher Level Personnel (CAPES) for the scholarships, the State University of Amapá (UEAP), Federal Rural University of Amazonia (UFRA), and to the Brazilian Agricultural Research Corporation (EMBRAPA), for the analyses and facilities.

## ORCID

Dhimitrius Neves Paraguassú Smith de Oliveira  <http://orcid.org/0000-0001-8709-385X>

Jefferson Bezerra Bezerra  <http://orcid.org/0000-0001-9371-7569>

Nilson Santos Ferreira  <http://orcid.org/0000-0002-8421-2558>

Wardsson Lustrino Borges  <http://orcid.org/0000-0002-2960-0638>

Lina Bufalino  <http://orcid.org/0000-0002-7688-3140>

Tiago Marcolino Souza  <http://orcid.org/0000-0002-4568-7884>

## References

- Abdul Khalil, H. P. S., M. S. Alwani, M. N. Islam, S. S. Suhaily, R. Dungani, Y. M. H'ng, and M. Jawaid. 2015. The use of bamboo fibres as reinforcements in composites. In *Biofiber reinforcements in composite materials*, ed. O. Faruk and M. Sain, 488–524. Cambridge: Woodhead Publishing.
- Al-Oqla, F. M., and S. M. Sapuan. 2014. Natural fiber reinforced polymer composites in industrial applications: Feasibility of date palm fibers for sustainable automotive industry. *Journal of Cleaner Production* 66:347–54. doi:10.1016/j.jclepro.2013.10.050.
- Aranda, M. A. G., A. G. De la Torre, and L. León-Reina. 2019. Powder-diffraction characterization of cements. *International Tables for Crystallography* H:855–867. doi:10.1107/97809553602060000986.
- Associação Brasileira de Normas Técnicas (ABNT). 1991. NBR 5733: Cimento Portland de alta resistência inicial. Rio de Janeiro.
- Associação Brasileira de Normas Técnicas (ABNT). 2003. NBR 11941: Madeira - Determinação da densidade básica. Rio de Janeiro.
- Barneto, A. G., C. Vila, and J. Ariza. 2011. Eucalyptus kraft pulp production: Thermogravimetry monitoring. *Thermochimica Acta* 520 (1–2):110–20. doi:10.1016/j.tca.2011.03.027.
- Berto, G. L., and V. Arantes. 2019. Kinetic changes in cellulose properties during defibrillation into microfibrillated cellulose and cellulose nanofibrils by ultra-refining. *International Journal of Biological Macromolecules* 127:637–48. doi:10.1016/j.ijbiomac.2019.01.169.
- Besbes, I., M. R. Vilar, and S. Bouf. 2011. Nanofibrillated cellulose from TEMPO oxidized eucalyptus fibres: Effect of the carboxyl content. *Carbohydrate Polymers* 84 (3):975–83. doi:10.1016/j.carbpol.2010.12.052.
- Bilba, K., and M. A. Arsene. 2008. Silane treatment of bagasse fiber for reinforcement of cementitious composites. *Composites. Part A, Applied Science and Manufacturing* 39 (9):1488–95. doi:10.1016/j.compositesa.2008.05.013.
- Bufalino, L., A. R. Sena Neto, G. H. D. Tonoli, A. De Souza Fonseca, T. G. Costa, J. M. Marconcini, J. L. Colodette, C. R. G. Labory, and L. M. Mendes. 2015. How the chemical nature of Brazilian hardwoods affects nanofibrillation of cellulose fibers and film optical quality. *Cellulose* 22 (6):3657–72. doi:10.1007/s10570-015-0771-3.

- Cai, M., H. Takagi, A. N. Nakagaito, Y. Li, and G. I. N. Waterhouse. 2016. Effect of alkali treatment on interfacial bonding in abaca fiber-reinforced composites. *Composites. Part A, Applied Science and Manufacturing* 90:589–97. doi:10.1016/j.compositesa.2016.08.025.
- César, A. A. S., L. Bufalino, A. S. Tahara, R. G. A. Mesquita, T. M. Souza, L. M. F. Andrade, F. A. Mori, and L. M. Mendes. 2019. Pretreated unbleached cellulose screen reject for cement-bonded fiberboards. *European Journal of Wood and Wood Products* 77 (4):581–91. doi:10.1007/s00107-019-01422-x.
- Chen, W. S., H. Yu, Y. Liu, Y. Hai, M. Zhang, and P. Chen. 2011. Isolation and characterization of cellulose nanofibers from four plant cellulose fibers using a chemical-ultrasonic process. *Cellulose* 18 (2):433–42. doi:10.1007/s10570-011-9497-z.
- Chikouche, M. D. L., A. Merrouche, A. Azizi, M. Rokbi, and S. Walter. 2015. Influence of alkali treatment on the mechanical properties of new cane fibre/polyester composites. *Journal of Reinforced Plastics and Composites* 34 (16):1329–39. doi:10.1177/0731684415591093.
- Ciolacu, D., F. Ciolacu, and V. I. Popa. 2011. Amorphous cellulose-structure and characterization. *Cellulose Chemistry and Technology* 45:13–21.
- Corrêa, A. C., E. D. M. Teixeira, L. A. Pessan, and L. H. C. Mattoso. 2010. Cellulose nanofibers from curaua fibers. *Cellulose* 17 (6):1183–92. doi:10.1007/s10570-010-9453-3.
- Faruk, O., A. K. Bledzki, H. P. Fink, and M. Sain. 2014. Progress report on natural fiber reinforced composites. *Macromolecular Materials and Engineering* 299:9–26. doi:10.1002/mame.201300008.
- Ferraz, J. M., C. H. S. Del Menezzi, M. R. Souza, E. Y. A. Okino, and S. A. Martins. 2012. Compatibility of pretreated coir fibres (*Cocos nucifera* L.) with Portland cement to produce mineral composites. *International Journal of Polymer Science* 2012:1–7. ID 290571. doi:10.1155/2012/290571.
- French, A. D. 2014. Idealized powder diffraction patterns for cellulose polymorphs. *Cellulose* 21 (2):885–96. doi:10.1007/s10570-013-0030-4.
- Garcez, M. R., E. O. Garcez, A. O. Machado, and D. A. Gatto. 2016. Cement-wood composites: Effects of wood species, particle treatments and mix proportion. *International Journal of Composite Materials* 6 (1):1–8. doi:10.5923/j.comaterials.20160601.01.
- Gartner, E. M., J. F. Young, D. A. Damidot, and I. Jawed. 2002. Hydration of Portland cement. In *Structure and performance of cements*, ed. P. Barnes and J. Bensted, 57–113. London: Spon Press.
- Gutiérrez, M. C., P. D. T. Rosa, M. A. de Paoli, and M. I. Felisberti. 2012. Biocompósitos de acetato de celulose e fibras curtas de Curauá tratadas com CO<sub>2</sub> supercrítico. *Polímeros* 22 (3):295–302. doi:10.1590/S0104-14282012005000037.
- Hachmi, M. H., M., G. A. Hakam, A. Sesbou, and A. Sesbou. 2017. Wood-cement inhibition revisited and development of new wood-cement inhibitory and compatibility indices based on twelve wood species. *Holzforschung* 71 (12):991–98. doi:10.1515/hf-2017-0022.
- Hajiha, H., and M. Sain. 2015. The use of sugarcane bagasse fibres as reinforcements in composites. In *Biofiber reinforcements in composite materials*, ed. O. Faruk and M. Sain, 525–49. Cambridge: Woodhead Publishing.
- Indran, S., and R. E. Raj. 2015. Characterization of new natural cellulosic fiber from *Cissus quadrangularis* stem. *Carbohydrate Polymers* 117:392–99. doi:10.1016/j.carbpol.2014.09.072.
- Ioelovich, M. 2008. Cellulose as nanostructured polymer: Short Review. *BioResources* 3:1401–18.
- Juenger, M. C. G., and H. M. Jennings. 2002. New insights on the effects of sugar on the hydration and microstructure of cement pastes. *Cement and Concrete Research* 3 (3):393–96. doi:10.1016/S0008-8846(01)00689-5.
- Kaushik, V. K., A. Kumar, and S. Kalia. 2012. Effect of mercerization and benzoyl peroxide treatment on morphology, thermal stability and crystallinity of sisal fibers. *International Journal of Textile Science* 1 (6):101–05. doi:10.5923/j.textile.20120106.07.
- Khan, J. A., and M. A. Khan. 2015. The use of jute fibers as reinforcements in composites. In *Biofiber reinforcements in composite material*, ed. O. Faruk and M. Sain, 3–34. Cambridge: Woodhead Publishing.
- Klemm, D., B. Heublein, H. P. Fink, and A. Bohn. 2005. Cellulose: Fascinating biopolymer and sustainable raw material. *Angewandte Chemie* 44 (22):3358–93. doi:10.1002/anie.200460587.
- Kocak, D., and S. I. Mistik. 2015. The use of palm leaf fibres as reinforcements in composites. In *Biofiber reinforcements in composite materials*, ed. O. Faruk and M. Sain, 273–81. Cambridge: Woodhead Publishing.
- Leão, A. L., I. S. Machado, S. F. Souza, and L. Soriano. 2007. Production of curaua (*Ananas erectifolius* L.B. Smith) fibers for industrial applications: Characterization and micropropagation. *Acta Horticulturae* 822:227–38. doi:10.17660/ActaHortic.2009.822.28.
- Li, X., L. G. Tabil, and S. Panigrahi. 2007. Chemical treatments of natural fiber for use in natural fiber-reinforced composites: A review. *Journal of Polymers and the Environment* 15 (1):25–33. doi:10.1007/s10924-006-0042-3.
- Luo, H., H. Zhang, L. Yue, A. Pizzi, and X. Lu. 2018. Effects of steam explosion on the characteristics of windmill palm fiber and its application to fiberboard. *European Journal of Wood and Wood Products* 76 (2):601–09. doi:10.1007/s00107-017-1259-7.
- Macêdo, A. N., A. A. C. Souza, and B. B. P. Neto. 2012. Chapas de cimento madeira com resíduos de indústria madeireira da região Amazônica. *Ambiente Construído* 12 (2):131–50. doi:10.1590/S1678-86212012000200009.
- Mansaray, K. G., and A. E. Ghaly. 1998. Thermal degradation of rice husks in nitrogen. *Bioresource Technology* 65 (1–2):13–20. doi:10.1016/S0960-8524(98)00031-5.

- Martins, M. A., P. K. Kiyohara, and I. Joékes. 2004. Scanning electron microscopy study of raw and chemically modified sisal fibers. *Journal of Applied Polymer Science* 94 (6):2333–40. doi:10.1002/app.21203.
- Mohanty, A. K., M. Misra, and L. T. Drzal. 2005. *Natural fibers, biopolymers, and biocomposites*. Boca Raton: CRC Press.
- Morán, J. I., V. A. Alvarez, V. P. Cyras, and A. Vázquez. 2008. Extraction of cellulose and preparation of nanocellulose from sisal fibers. *Cellulose* 15 (1):149–59. doi:10.1007/s10570-007-9145-9.
- Na, B., Z. Wang, H. Wang, and X. Lu. 2014. Wood-cement compatibility review. *Wood Research* 59:813–26.
- Oksman, K., A. P. Mathew, D. Bondeson, and I. Kvien. 2006. Manufacturing process of cellulose whiskers/poly(lactic acid) nanocomposites. *Composites Science and Technology* 66 (15):2776–84. doi:10.1016/j.compscitech.2006.03.002.
- Oliveira, D. N. P. S., P. I. C. Claro, R. R. Freitas, M. A. Martins, T. M. Souza, B. M. Silva E Silva, L. M. Mendes, and L. Bufalino. 2019. Enhancement of the Amazonian Açai waste fibers through variations of alkali pretreatment parameters. *Chemistry Biodiversity* 16:e1900275. doi:10.1002/cbdv.201900275.
- Pacheco-Torgal, F., and S. Jalali. 2011. Cementitious building materials reinforced with vegetable fibres: A review. *Construction and Building Materials* 25 (2):575–81. doi:10.1016/j.conbuildmat.2010.07.024.
- Paula, J. E. 1975. Anatomia de *Euterpe oleracea* Mart. (Palmae da Amazônia). *Acta Amazonica* 5 (3):265–78. doi:10.1590/1809-43921975053265.
- Pedrazzi, C., J. L. Colodette, R. C. D. Oliveira, and V. K. D. Wille. 2013. Morphologic evaluation of Eucalyptus kraft pulp fibers with different xylans contents. *Scientia Forestalis* 41:515–22.
- Rokbi, M., H. Osmani, A. Imad, and N. Benseddiq. 2011. Effect of chemical treatment on flexure properties of natural fiber reinforced polyester composite. *Procedia Engineering* 10:2092–97. doi:10.1016/j.proeng.2011.04.346.
- Rowell, R. M., J. S. Han, and J. S. Rowell. 2000. Characterization and factors effecting fiber properties. In *Natural polymers and agrofibers based composites*, ed. E. Frollini, A. L. Leao, and H. C. Luiz, 115–34. Mattoso: Embrapa Instrumentação Agropecuária.
- Sena Neto, A. R., M. A. Araujo, F. V. Souza, L. H. Mattoso, and J. M. Marconcini. 2013. Characterization and comparative evaluation of thermal, structural, chemical, mechanical and morphological properties of six pineapple leaf fiber varieties for use in composites. *Industrial Crops and Products* 43:529–37. doi:10.1016/j.indcrop.2012.08.001.
- Sgriccia, N., M. Hawley, and M. Misra. 2008. Characterization of natural fiber surfaces and natural fiber composites. *Composites. Part A, Applied Science and Manufacturing* 39 (10):1632–37. doi:10.1016/j.compositesa.2008.07.007.
- Vo, L. T. T., and P. Navard. 2016. Treatments of plant biomass for cementitious building materials - A review. *Construction and Building Materials* 121:161–76. doi:10.1016/j.conbuildmat.2016.05.125.
- Wilson, L., Y. W. Weihong, W. Blasiak, G. R. John, and C. F. Mhilu. 2011. Thermal characterization of tropical biomass feedstocks. *Energy Conversion and Management* 52 (1):191–98. doi:10.1016/j.enconman.2010.06.058.
- Yan, L., N. Chouw, and X. Yuan. 2012. Improving the mechanical properties of natural fibre fabric reinforced epoxy composites by alkali treatment. *Journal of Reinforced Plastics and Composites* 31 (6):425–37. doi:10.1177/0731684412439494.
- Yan, L., B. Kasal, and L. Huang. 2016. A review of recent research on the use of cellulosic fibres, their fibre fabric reinforced cementitious, geo-polymer and polymer composites in civil engineering. *Composites Part B: Engineering* 92:94–132. doi:10.1016/j.compositesb.2016.02.002.
- Zhao, Y., Y. Wang, J. Y. Zhu, A. Ragauskas, and Y. Deng. 2008. Enhanced enzymatic hydrolysis of spruce by alkaline pretreatment at low temperature. *Biotechnology and Bioengineering* 99 (6):1320–28. doi:10.1002/bit.21712.